



Removal of Tetracycline from Wastewater Using Circulating Fluidized Bed

Sabreen Lateef Kareem^a and Ahmed A Mohammed^b

^aEnvironmental Planning Department, College of Physical Planning, University of Kufa, Iraq

^bEnvironmental Engineering Department, College of Engineering, University of Baghdad, Baghdad, Iraq

Abstract

In this study, the circulating fluidized bed was used to remove the Tetracycline from wastewater utilizing a pistachio shell coated with ZnO nanoparticles. Several parameters including, Tetracycline solution flowrate, initial static bed height, Tetracycline initial concentration and airflow rate were systematically examined to show their effect on the breakthrough curve and the required time to reach the adsorption capacity and thus draw the fully saturated curve of the adsorbent. Results showed that using ZnO nanoparticles will increase the adsorbent surface area and pores and as a result the adsorption increased, also the required time for adsorbent saturation increased and thus the removal efficiency may be achieved at minimum antibiotic flowrate, maximum bed height, higher antibiotic concentration, and higher airflow rate. Also, a minimum fluidization velocity correlation was developed in this study. This correlation was found to be a function of liquid velocity, bed height, particle size, and particle density. The results showed that circulating fluidized bed has a better performance and last more than two hours before the bed biomass exhausted in comparison with traditional fluidized bed.

Keywords: Tetracycline, Circulating Fluidized Bed, Minimum fluidization velocity, Bed height, Breakthrough curve

Received on 13/12/2019, Accepted on 23/01/2020, published on 30/09/2020

<https://doi.org/10.31699/IJCPE.2020.3.4>

1- Introduction

Contamination of water resources by toxic chemicals is one of the community's greatest environmental challenges, especially when these resources were the only viable drinking water source [1], [2]. Antibiotics are highly consumed compounds among pharmaceutical drugs due to their efficacy in the treatment of a wide range of bacterial infections in human, livestock, poultry and fish [3]. Antibiotics considers as a special medicines because it can affect pathogenic bacteria when leaving human tissues and cells unused [4], [5]. It is very important to remove antibiotic residues before discharging sewage into the atmosphere because some types of them are persist and can be toxic for aquaculture, but it usually involves high costs [6]. Advance oxidation process (AOP) can transform or even fully mineralize antibiotic molecules into simple compounds, but the some disadvantage of these process were high cost and difficult to remove completely on an industrial scale [7].

As a result, physicochemical technologies prove to be a highly appropriate treatment choice for organic waste product [8]. Adsorption process is very effective, operates simply and is relatively inexpensive [9].

Adsorption method is commonly used to eliminate organic chemicals in polluted sites using suitable adsorbents [8].

Recently, agricultural wastes have attracted great attention from researchers in their initial or modified forms to be used as adsorbents in treatment systems'. Because of their minimal cost and widespread existence in nature, such pistachio shells, banana peels, hazelnut straws, walnut shells orange peels, rice husks, oat hulls and ground nut shells [10].

The removal of contaminants using nanoparticles has emerged as an interesting area of research due to their unique properties. Also, they offer opportunities for higher efficiency and cost-effectiveness due to the higher surface area and higher active sites that modify any material during nanocomposite preparation [11].

The most effective method is maximizing the adsorbent mechanical strength by coating the surface with nanoparticles which also increasing the adsorbent surface area and adsorption ability [12]. The nanoparticles adsorbents used primarily for treating wastewater are synthesized from silver, alumina, zinc oxide, copper oxide iron oxide, titanium oxide, stannous oxide and some alloys [13].

Some undesirable problems of pure nanoparticles as adsorbents are expensive needs advance filtration procedure for separation from aqueous liquids and large agglomeration tendency which reduce the reactivity in traditional treatment methods [14].

So, traditional adsorbents coated with nanoparticles are an effective alternate in avoiding the difficulties of using pure nanomaterial and increasing the main adsorbents efficiency to remove pollutants from different origins [15]. Zinc oxide (ZnO) nanoparticles can be used as essential adsorbent for the removing of antibiotics due to the low production costs and the opportunity for using in diverse fields [16]. A new form of reactor known as gas, liquid and solid circulating fluidized beds (GLSCFBs) has been used, in which the adsorbent is circulated between the downer and the riser [17]. GLSCFBs providing extra advantages to the old-style fluidized bed which include, high contact efficiency between liquid–solid, operated continuously because adsorption and desorption work simultaneously that the particles circulated between two separate columns [18] reduced back mixing of phases, greater throughput and improved mass transfer owing to the higher velocity and uniform flow pattern [19].

To the best of our knowledge ,no research investigated the efficiency of pistachio shell (PIS) coated with ZnO nanoparticles (CPS) for the elimination of antibiotic from wastewater .So that this work aims to examine the capability of CPS for treatment of wastewater contaminated with TEC by circulated fluidized bed.

2- Materials Preparation

2.1. Chemicals

Powdered TEC, purity: 98%, were taken from General Company for drugs industry (Samarra, Iraq) without more purification. Stock solution of TEC, was prepared by dissolving a suitable amount (according to concentration required) of powdered TEC in 1 L of distilled water. Due to the laboratory instability conditions, solution should be prepared daily at the experiments time. ZnONP was solid, white odorless powder with density equal to 5600 kg/m³ and MW=81.4 g/mol. Table 1 displays the properties of TEC and ZnO nanoparticles.

2.2. Adsorbent Preparation

CPS was prepared as follow.

- 1- PIS shells were locally collected, cleaned, washed with distilled water for 2–3 hours, and then dried at 105 °C using suitable oven for 24 hrs.
- 2- The dried PIS shell prepared were grinding and sieved. Some PIS prepared amounts were characterized, and the residual was stored for the ZnO nanoparticles ZnONP surface coating.
- 3- ZnONP obtained from Xi'an Lyphar Biotec Co., Ltd, China. PIS coating with the ZnONP was done using an ultrasonic device.
- 4- The ZnONP were mixed with acetone as a suitable dispersant in an ultrasonic for 30 min. and then the prepared PIS were added in different mass and shaken for 2 hrs to obtain CPS
- 5- Finally, the dried CPS was kept in stoppered containers to be used in the necessary experiments. Fig. 1 shows the CPS preparation. .

Table 1. Main characteristics of antibiotics studied

Compound	Abbr.	Formula	MW (g/mol)	pKa	Chemical structure
Tetracycline	TEC	C ₂₂ H ₂₄ N ₂ O ₈	480.9	pKa1 = 3.3 pKa2 = 7.7 pKa3 = 9.27	

2.3. Adsorbent Characterization Techniques

An X-Ray diffractometer (XRD) was used to obtain XRD patterns of the PIS, ZnO and CPS crystalline structure in range of 2θ from 20° to 80°, with a step width of 0.02° and scan rate of 1° / second. In another hand, Scanning Electron Microscopy (SEM) images were conducted to detect the changes in the surface morphology that occur due to the adsorption process. The specific surface area SBET of the samples were carried out by a Micrometrics instrument company, USA, ASAP2020 giving to the BET (Brunauer, Emmet and Teller) model

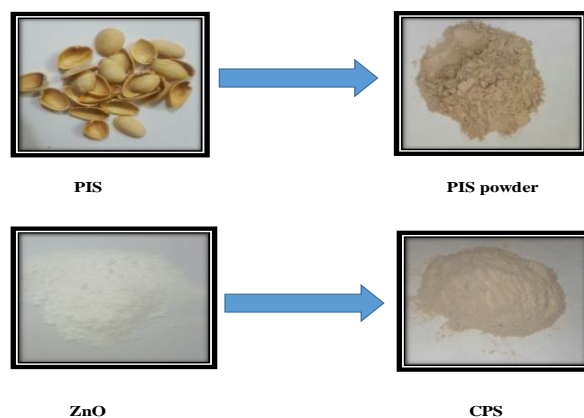


Fig. 1. Preparation of CPS

Table 2. Parameters range tested in CFB

Parameters	Range	Purpose	
Continuous	Liquid flow rate (L/hr)	18, 21 and 24	To find optimum flow rate and to find the effect of flow rate on breakthrough curves.
	Bed height, cm	2, 4 and 6	To study the effect of CPS bed height on Breakthrough curves.
	Initial concentration, mg/L	10,30 and 50	To study the effect of TEC initial concentration on breakthrough curves
	Air flow rate (cc/min)	400, 600 and 800	To find the optimum air flow rate for fluidization.

2.4. Circulating Fluidized Bed

Fig. 2 show the schematic diagram for CFB column used in removal of TEC from wastewater and Table 2 represents the major parameters examined.

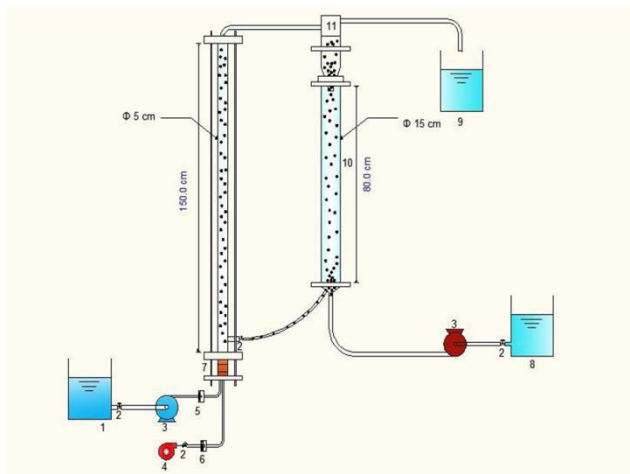


Fig. 2. GLSCFB schematic diagram 1: Feeding tank, 2: Valve, 3: Pump, 4: Air compressor, 5: Flow meter of liquid, 6: Gas flow meter, 7: Distributer, 8: Distilled water for the downer 9: Treated wastewater, 10: Downer column, 11: Solid-liquid separator, 12: Riser column.

3- Results and Discussion

3.1. X-Ray Diffraction Characterization

XRD analysis results of CPS, ZnO, and PIS and in the range of 5-60° are depicted in Fig.3. XRD of ZnO in Fig.3A which show that 100% percent of material was ZnO and hexagonal structure also this result was proved by comparing given material XRD peaks with standard ZnO XRD card, average diameter size of ZnONP calculated using (Debye-Scherrer formula) Eq.1 [14].

$$d = \frac{0.89\lambda}{b\cos\theta} \quad (1)$$

Where: d, represents the crystallite size, b, refers to the full-width at half maximum (FWHM) in radians, $\lambda=0.15406$ nm is the wavelength and θ is the half diffraction angle of 2θ . By applying Eq.1 ZnONP diameter were found to be 20.9 nm.

Fig. 3 b and c depicts XRD forms of PIS and CPS, respectively. The PIS XRD analysis Fig. 3 b displays that the PIS main ingredients were cristobalite (97.4%), and periclase (2.6%). XRD analysis of CPS displays the forming of new peaks as seen in Fig. 3 c owing to the newly resulted ZnONP layers. However, peak diffraction is observed at “((20)) = 31.7288, 34.3877, 36.2432, 47.5063, 56.5137 and 62.8756, which related to the reflection from (100), (002), (101), (102), (110) and (103) planes, respectively”.

These were owing to the ZnO layer (84.3%) and similarly showed that the shells of the PIS were shielded with pure ZnONP [5]-[20], standard XRD card of ZnO shown in Fig. 4.

3.2. Scanning Electron Microscopy (SEM)

The SEM analysis was conducted to investigate the shape and surface morphology of the natural PIS, CPS and CPS loaded with antibiotics. The representative images are shown in Fig. 5 (a-c). The surface morphology of natural pistachio shell before preparation of the composite was shown in Fig. 5 a, this figure shows that the PIS surface was coarse, regular with spherical irregular aggregates. Numerous small pores and cavities were detected making PIS a good supportive surface for ZnONP. The SEM of the CPS Fig. 5 b indicated that the CPS surface is coarse; as well as it contains several non-uniformly and separated aggregates. So, there are many great ravines and extended grooves in the CPS outer wall.

These CPS surface morphological characteristics, represents as a positive instant provide surface area for TEC molecules sorbing. In this direction, the specific surface area of PIS was determined to be equal to 0.972 m²/g, which was significantly increased after coating with ZnO nanoparticles to be equal to 4.234 m²/g these allowing TEC molecules to enter and interact with surface functional groups. Comparing Fig. 5 b and CPS SEM image after TEC adsorption Fig. 5 c, the morphological properties of CPS was significantly altered during the TEC adsorption. the CPS surface become bright and smoother, and several pre-separated aggregates are coalesced as pore surfaces were entirely filled with TEC molecules, this remark states that TEC were adsorbed onto the active surface groups exist inside the pores and the well-formed pores on the CPS may be the main reason behind the high antibiotics uptake [21], [22].

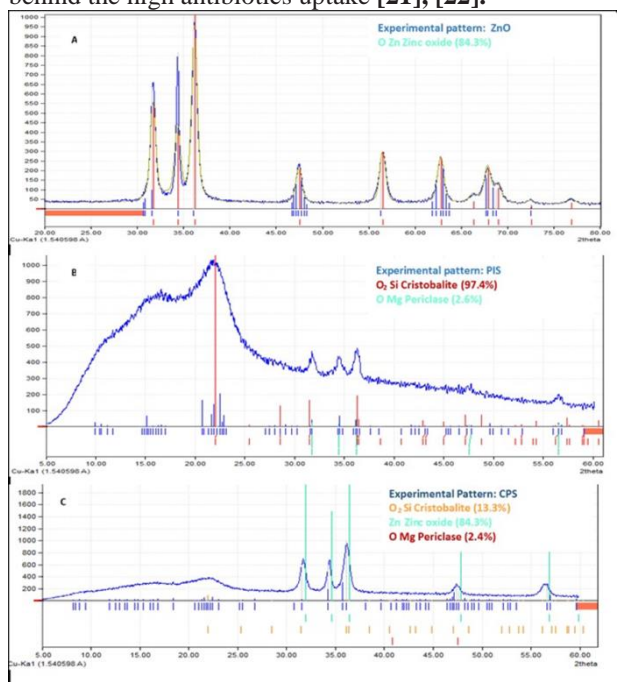


Fig. 3. XRD forms of the (A) ZnO (B) PIS and (C) CPS

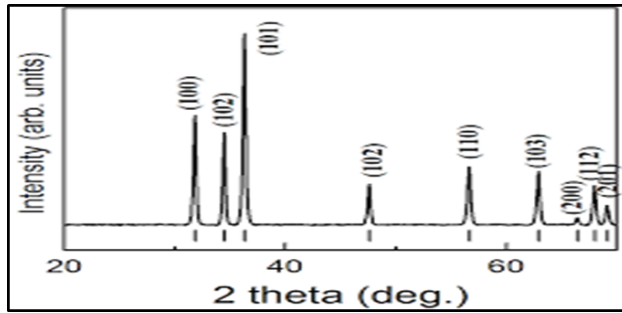


Fig. 4. XRD standard card of ZnO nanoparticles

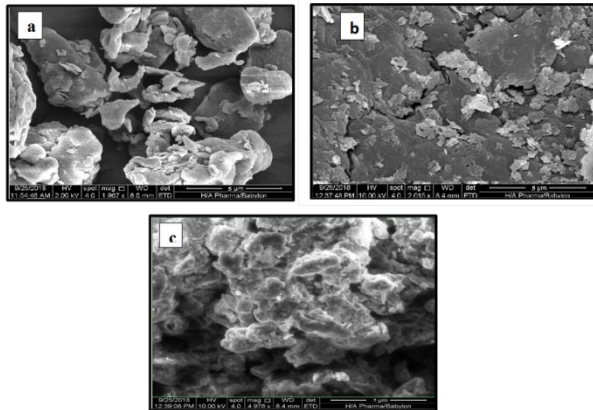


Fig. 5. SEM pictures of (a) PIS (b) CPS and (c) CPS after TEC adsorption

3.3. Continuous Mode Experiments

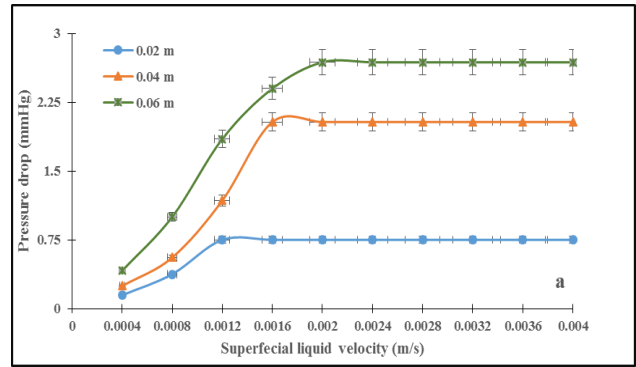
a. Minimum fluidization velocity (U_{lmf})

The minimum fluidization velocity (U_{lmf}) in the instance of gas-liquid-solid fluidization (GLSF) and liquid represents a continuous phase usually defined as the superficial velocity of liquid (U_L) at which the bed looks fluidized for a known superficial velocity of gas (U_g) [23] U_{lmf} required to attain fluidization obtained from the bed pressure drop (Pd) against U_L scheme at a constant U_g . U_{lmf} in this study has been obtained as displayed in Fig. 6 a-c. From Fig. 6 a, it is noticed that initial static bed height H_s affect U_{lmf} , when H_s increase, pressure drop increase then U_{lmf} increase [24].

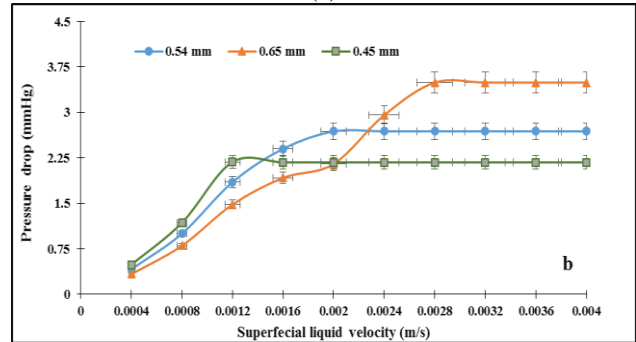
This is due to that fluidization bed is achieved when the upward drag and inertial forces applied by the fluids on the particles equals to the bed buoyant weight, the effect of initial static bed height H_s on the U_{lmf} only be expected [25].

From Fig. 6 b, it is noticed that U_{lmf} rises with increasing particle size(dp) increase. U_g also affect U_{lmf} , U_{lmf} reduces as U_g increased which confirming that bubbles support fluidization.

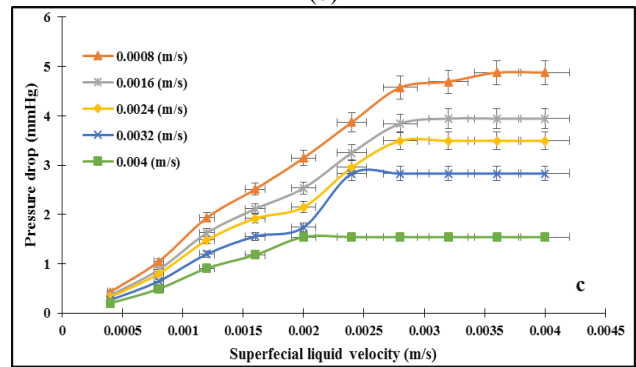
The rate of U_{lmf} is decreasing usually high at lower U_g values and low as gas velocity increasing. Also at higher U_g , the U_{lmf} becomes nearly constant Fig. 6 c [23].



(a)



(b)



(c)

Fig. 6. Pressure drop Variant with U_L for a) different H_s value at $dp = 0.54\text{mm}$ and $U_g = 0.0024\text{ m/s}$, b) for different dp at $H_s = 0.06\text{m}$ and $U_g = 0.0024\text{ m/s}$, and c) for different U_g value at $dp = 0.65\text{ mm}$ and $H_s = 0.06\text{ m}$

The experimental data for minimum liquid fluidization velocity are presented in Table 3 , and can be correlated by non-linear regression analysis as illustrated in Eq.2 which can be used in similar systems for the prediction of U_{lmf} with coefficient of determination (R^2) = 0.9789 Fig. 7.

Eq. 2 can applied in Reynolds number (Re) range (0.45-3.25) which is calculated by Eq.3.From Eq.2, it can be concluded that the particle size has a larger effect than other parameters on minimum fluidization velocity and as the U_g increased, U_{lmf} decreased due to the effect of U_g of particle on fluidization

$$U_{lmf} = 0.00184 U_g^{-0.343} dp^{1.198} H_s^{0.484} \rho_s^{-0.351} \quad (2)$$

$$Re = \frac{\rho V d}{\mu} \quad (3)$$

Table 3. Experimental data obtained and correlated for Ulmf correlation

Ulmf ^{exp} (m/s)	dp(mm)	Ug(m/s)	Hs(m)	Density(kg/m ³)	SSE
0.0012	0.54	0.0024	0.02	0.715	5.6178E-10
0.0016	0.54	0.0024	0.04	0.715	2.0222E-09
0.002	0.54	0.0024	0.06	0.715	2.1992E-12
0.0016	0.45	0.0024	0.06	0.7482	2.7828E-10
0.0024	0.65	0.0024	0.06	0.6824	1.9765E-08
0.0036	0.65	0.0008	0.06	0.6824	1.0273E-08
0.0032	0.65	0.0016	0.06	0.6824	7.8901E-08
0.0024	0.65	0.0032	0.06	0.6824	9.5688E-09
0.002	0.65	0.004	0.06	0.6824	1.7629E-08

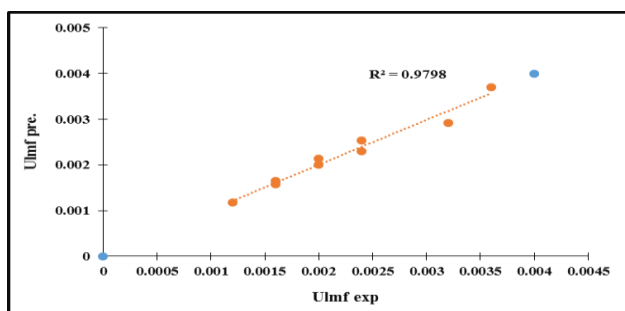


Fig. 7. Comparison between experimental and predicted Ulmf

Since 0.54 mm CPS particle size was used in continuous system and as shown in Table 3, the minimum bed required to fluidized this size was 0.002m/s (250 cc/min) (15 L/hr) at air velocity 0.0024 m/s (300cc/min). Therefore 18 L/hr was the minimum water flow rate tested in continuous experiments, flow rates upper than the minimum examined to rise the mixing and studying its influence on the antibiotics removal efficiency.

b. Breakthrough Curves

By plotting C/C_0 versus time for TEC, the breakthrough curves for each antibiotic were obtained.

b1. Effect of Liquid Flow Rate

Steeper breakthrough curves resulted with increasing flow rate because as the flow rate become high, the residence time for TEC in column become shorter. Also, there is a possibility for TEC to remain in the outlet stream from the column before equilibrium achieved because of contact time reduction. The results showing the effect of liquid flow rate on the removal efficiency of TEC are plotted in Fig.8. The liquid phase residence time decreases with a UL increase, (breakthrough time for 18, 21, and 24 l/hr flowrate was 380, 340, and 300 min respectively) thus adsorption time reduced and higher pollutant concentration noticed in raffinate stream. These results agree with that obtained by [26]. 18 l/hr. was chosen as the best solution flow rate for the next experiments.

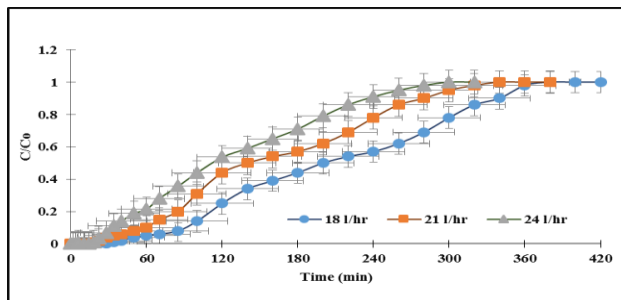


Fig. 8. Effect of flow rate on removal of TEC at initial conditions 6 cm, 10 ppm, and 600cc/min

b2. Effect of Cps Bed Height (Hs)

The bed height is considered as a major adsorption process design factor and its effect was studied. The experimental breakthrough curves are present in Fig.9.

These figures show that by increasing bed height, the time needed to reach equilibrium increased because long contact time occurred between contaminants solution and particles (breakthrough time for 6, 4 and 2 cm was 380,340 and 320 min, respectively). Small bed heights will be saturated in shorter time; this displays that at small bed height the concentration ratio of adsorbate waste rises faster than that for a longer bed height.

Besides, as bed height increased, the surface area or sorption sites increase improving the sorption process. In the case of constant flow rate, Increasing H_s will increase the TEC solution contact time, and improve the TEC removal efficiency [27]. So, 6 cm bed height was chosen as the optimum value for the next experiments.

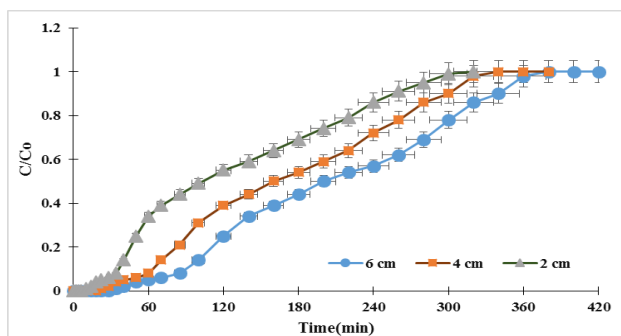


Fig. 9. Bed height effect on removal efficiency of TEC at initial conditions 18 l/hr, 10 ppm, and 600cc/min

b3. Influence of Initial Concentration

The effect of different initial antibiotic concentrations (10, 30 and 50 ppm) was examined at constant water and air flow rate and bed height.

The experimental breakthrough curves resulted are illustrated in Fig. 10 for antibiotics adsorption in terms of C/C_0 versus time. In this figure, it is obvious that saturation time decreases with increasing an initial concentration and inverse relation between the breakpoint and initial concentration (breakthrough time for 10, 30 and 50 ppm was 380,280 and 220min). Low initial solute concentration make the saturation time of diffusion rate longer.

As the TEC influent concentration increases, the adsorption capacity also increases. This is attributed to a high concentration difference (driving force for adsorption) between in liquid and solid phase also, may increase solute mass transfer rate to contact adsorbent active free sites. If the initial antibiotic concentration is high, faster bed saturation occurring and the slope of the breakthrough curve is higher, so 10 ppm initial antibiotic solution concentration was chosen as the best value for the next experiments [26], [27].

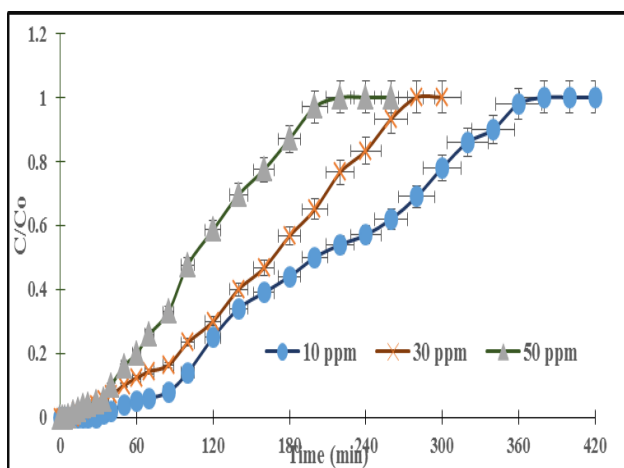


Fig. 10. Effect of initial concentration on removal efficiency of (a) TEC, (b) CIP and (c) AMO at initial conditions 18 l/hr, 6 cm, and 600cc/min

b4. Air Flow Rate Effect

Fig. 11 shows the effect of air flow rate variation (400cc/min, 600cc/min and 800cc/min) on breakthrough curve. The breakthrough curve plot obtained at 800cc/min displays a sharper shape compared with lower air flow rate curve. This is due to that long time is required to reach saturation in the case of high air flow rate which is because of more turbulent flow that reduces the resistance of mass transfer. Breakthrough time for 400,600 and 800 cc/min was 360,340 and 280 min, respectively [28].

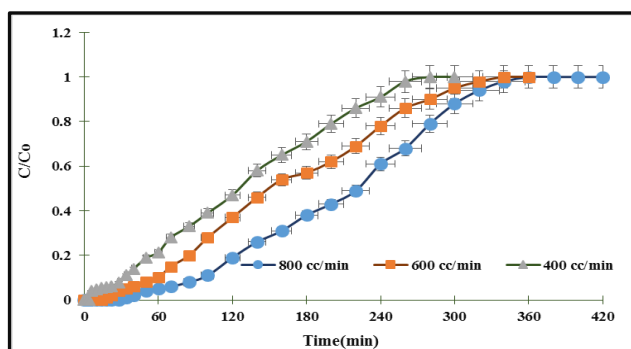


Fig. 11. Effect of air flow rate on breakthrough curve of TEC, at initial conditions 18 l/hr, 6 cm, and 10 ppm

c. Comparison between Traditional Fluidized Bed and Circulated Fluidized Bed

The difference between traditional fluidized beds (conventional) vs. the circulated fluidized bed (CFB) is shown in Fig. 12. The same conditions were used for each system, 10 mg/L as TEC concentration, (6 cm) for bed height, 18 L/hr. as liquid flow rate, and 400cc/min as gas flow rate. The results obtained show the efficiency of CFB on the removal of TEC. So the CFB has better result and last for more than 2 hours before the CPS exhausted. In a CFB, solid particles are circulated between the riser and the downer at higher velocities compared to conventional fluidized beds, which leads to better contacting efficiency between phases, and higher mass transfer can be achieved with CFBs, which makes this type of reactor more preferable over the conventional fluidized beds.

It has also been reported that the GLSCFB provides higher gas holdup, more uniform bubble sizes, better interphase contact, and more efficient heat transfer into or out of the bed. For some gas-liquid-solid reaction systems, solid adsorbent lose their activity due to deposition of antibiotic.

On their surfaces, and need regeneration outside the bed. By using an accompanying down comer as a regenerator, both reaction and regeneration of the catalysts can be coupled by a continuous circulating operation. The liquid velocity is not enough to entrain the particles and wash them out of the column in conventional fluidization, while in circulated fluidized bed, the particles were carried to the top of the column by using high liquid velocity and then return them to the bottom by a recycle line or column [9].

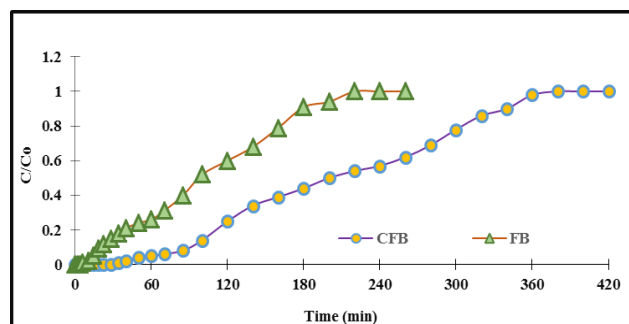


Fig. 12. Traditional fluidized bed (TFB) vs. CFB for the removal of TEC at initial conditions 18 L/hr as flow rate, 6 cm as bed height, 10 mg/L as initial concentration, and 800 cc/min as gas flow rate

4- Conclusion

CPS was found to be feasible media for use as a bed column for the removal of TEC from contaminated water. A fluidized -bed column was used to investigate the sorption of all antibiotics studied and it was depended on feed flow rate, initial antibiotics concentration and bed height of adsorbent. The minimum fluidization velocity of bed was affected by U_g , d_p , H_s and particle density.

The variation of liquid superficial velocity from 0.0024 to 0.0032 result an obvious depletion in sorption removal efficiency. The variation of bed height from 0.02 to 0.06 m for each antibiotics resulted in an obvious increase in time to reach C/Co equal to 1. Increasing initial contaminant concentration causes a decrease in biosorption capacity and increasing the time required for CPS to be fully saturated. Finally, increasing air flow rate increase the time required for CPS to reach saturated.

Nomenclature

Abbreviation	Description
CPS	Pistachio shell coated with zinc oxide
dp	Particle diameter
GLSFB	Gas-Liquis-Solid Fluidized Bed
Hs	Bed height
Pd	Pressure drop
PIS	Pistachio shell
TEC	Tetracycline
Ug	Gas velocity
UL	Liquid velocity
Ulmf	Minimum fluidization velocity

References

- [1] [H.M.Selman, A.A.Mohammed, Removal of copper ions from aqueous solution using liquid-surfactant-membrane technique, Iraqi Journal of Chemical and Petroleum Engineering 20 \(2019\) 31 – 37.](#)
- [2] [A.A. Al-Haleem, K. M Abed, Treating of oil-based drill cuttings by earthworms, Research Journal of Pharmaceutical, Biological and Chemical Sciences 7\(2014\) 2088-2094.](#)
- [3] [M.S. Legnoverde, S. Simonetti, E.I. Basaldella, Influence of pH on cephalixin adsorption onto SBA-15 mesoporous silica: Theoretical and experimental study. Applied Surface Science, 300\(2014\) 37-42.](#)
- [4] [A.W. Al-Shahwany, A. A. Al-Hemiri, K.M. Abed, Comparative evaluation of alkaloids extraction methods from the root bark of punica granatum linn. Advances In Bioresearch 4\(2013\)](#)
- [5] [A.A. Mohammed, S.L Kareem, Adsorption of tetracycline fom wastewater by using Pistachio shell coated with ZnO nanoparticles: Equilibrium, kinetic and isotherm studies. Alexandria Engineering Journal, 58\(2019\)917-928.](#)
- [6] [A. Watkinson, E.Murby, S. Costanzo, Removal of antibiotics in conventional and advanced wastewater treatment: implications for environmental discharge and wastewater recycling. Water Resources, 41 \(2007\) 4164-4176.](#)
- [7] [M. Mehrjouei, S. Müller, D.Möller, Energy consumption of three different advanced oxidation methods for water treatment: a cost-effectiveness study. Journal of Cleaner Production, 65\(2014\) 178–183.](#)
- [8] [V. Homem, L. Santos, Degradation and removal methods of antibiotics from aqueous Matrices—a review. Journal of Environmental Management, 92\(2011\) 2304–2347.](#)
- [9] [A.A.Najim, A.A. Mohammed, Biosorption of methylene blue from aqueous solution using mixed alga. 19\(2018\)1-11.](#)
- [10] [A.A. Mohammed, Biosorption of lead, cadmium, and zinc onto sunflower shell: equilibrium, kinetic, and thermodynamic studies, 16\(2015\)91-105.](#)
- [11] [M. Yang, J. He, X. Hu, C. Yan, Z. Cheng, CuO nanostructures as quartz crystal microbalance sensing layers for detection of trace hydrogen cyanide gas. Environmental Science and Technology, 45\(2011\) 6088-94.](#)
- [12] [Z.Chen, X. Jin, Z. Chen, M. Mallavarapu, R. Naidu, Removal of methyl orange from aqueous solution using bentonite-supported nanoscale zero-valent iron. Journal of Colloid and Interface science, 363\(2011\) 601–607.](#)
- [13] [J. Chen, W.Chen, D.Zhu, Adsorption of nonionic aromatic compounds to single walled carbon nanotubes: effects of aqueous solution chemistry. Environmental Science and Technology, 42\(2008\) 6862-6868.](#)
- [14] [A.A. Mohammed, T.J. Al-Musawi, S.L. Kareem, M. Zarrabi, A.M. Al-Ma'abreh, Simultaneous adsorption of tetracycline, amoxicillin, and ciprofloxacin by pistachio shell powder coated with zinc oxide nanoparticles, Arabian Journal of Chemistry \(2019\).](#)
- [15] [A.Mohseni-Bandpi, T. J. Al-Musawi, E. Ghahramani, M. Zarrabi, S.Mohebi S.A., Vahed, Improvement of zeolite adsorption capacity for cephalixin by coating with magnetic Fe₃O₄ nanoparticles. Journal of Molecular Liquid, 218 \(2016\), 615–624.](#)
- [16] [N.Dhiman, N. Sharma, Batch adsorption studies on the removal of ciprofloxacin hydrochloride from aqueous solution using ZnO nanoparticles and groundnut \(Arachis hypogaea\) shell powder: a comparison. Indian Chemical Engineer, \(2018\). 1–10.](#)
- [17] [Z.Liu, M. Vatanakul, L. Jia, Y. I. N. G. Zheng, Hydrodynamics and Mass Transfer in Gas-Liquid-Solid Circulating Fluidized Beds. Chemical engineering & technology, 26\(2003\)1247-1253.](#)
- [18] [Lan, Q., Bassi, A., Zhu, J. X. J., & Margaritis, A. \(2002\). Continuous protein recovery from whey using liquid-solid circulating fluidized bed ion exchange extraction. Biotechnology and bioengineering, 78\(2\), 157-163.](#)

- [19] [J.Mazumder, J. Zhu, A. S. Bassi, A. K. Ray, Modeling and simulation of liquid–solid circulating fluidized bed ion exchange system for continuous protein recovery. Biotechnology and bioengineering, 104\(2009\) 111-126. doi.org/10.1002/bit.22368](#)
- [20] [M.Ersana, U. A. Guler, U. Acikel, M.Sarioglu, Synthesis of hydroxyapatite/clay and hydroxyapatite/pumice composites for tetracycline removal from aqueous solutions, Process Safety and Environmental Protection 9\(2015\): 6 22–32](#)
- [21] [P.Chang, Z. Li, T.Yu, S. Munkhbayer, T. Kuo, Y.Hung, J. Jean, K.Lin, Sorptive removal of tetracycline from water by palygorskite, Journal of Hazardous Material, 165\(2009\) 148–155.](#)
- [22] [A.A. Mohammed, F. Brouers, I.S. Samaka, T.J. Al-Musawi, Role of Fe₃O₄ magnetite nanoparticles used to coat bentonite in zinc\(II\) ions sequestration, Environmental Nanotechnology, Monitoring & Management, 10\(2018\) 17–27.](#)
- [23] [L.A. Briens, N. Ellis, Hydrodynamics of three-phase fluidised bed systems examined by statistical, fractal, chaos and wavelet analysis methods. Chemical Engineering Science 60\(2005\) 6094–6106.](#)
- [24] [A. Delebarre, J. M.Morales, L.Ramos, Influence of bed mass on its fluidization characteristics,Chemical Engineering Journal 98\(2004\) 81-88.](#)
- [25] [H.M.Jena, Hydrodynamics of Gas-Liquid-Solid Fluidized and Semi-Fluidized Beds. PhD. Thesis, National Institute of Technology, Rourkela. \(2009\).](#)
- [26] [A. A. Mohammed, A.A. Najim, T.J. Al-Musawi, A.I. Alward, "Adsorptive performance of a mixture of three nonliving algae classes for nickel remediation in synthesized wastewater." *Journal of Environmental Health Science and Engineering* 17, no. 2 \(2019\): 529-538.](#)
- [27] [J.H. Al-Baidhani, S. T. Al-Salihy, Removal of heavy metals from aqueous solution by using low cost rice husk in batch and continuous fluidized experiments, International Journal of Chemical Engineering and Applications, 7\(2016\) 6-10](#)
- [28] [M. Loredó-Cancino, E. Soto-Regalado, R. B. García-Reyes, F. Cerino-Córdova J. de, M. T. Garza-González, M. M. Alcalá-Rodríguez, N. E. Dávila-Guzmán \(2014\). Adsorption and desorption of phenol onto barley husk-activated carbon in an airlift reactor. *Desalination and Water Treatment*, 57\(2\), 845–860.](#)
- [29] [F. Brouers, T.J. Al-Musawi, Brouers-Sotolongo fractal kinetics versus fractional derivative kinetics: a new strategy to analyze the pollutants sorption kinetics in porous materials. *Hazardous Material* ,350\(2015\)162-168.](#)

ازالة التتراسايكلين من المياه الملوثة باستخدام الابراج المتميعة الدوارة

صابرين لطيف كريم¹ و احمد عبد محمد²

¹قسم التخطيط البيئي/جامعة الكوفة

²قسم الهندسة البيئية/جامعة بغداد

الخلاصة

تم اعتماد برج الامتزاز المتميع الدوار لازالة التتراسايكلين بنظام مستمر باستخدام قشور الفستق المطلية باوكسيد الزنك النانوي كمادة مازة ، وتم فحص تأثيرات عوامل عدة بما في ذلك: معدل تدفق التتراسايكلين ، عمق الحشوة ، وتركيز التتراسايكلين الاولي ومعدل تدفق الهواء على منحنى الانكسار والوقت المطلوب للحشوة للوصول الى قابلية الامتزاز . اضافة اوكسيد الزنك يؤدي الى زيادة المساحة السطحية والفراغات في المادة المازة مما يؤدي الى زيادة الامتزاز وايضا الوقت اللازم المطلوب للوصول الى حد الاشباع ايضا يزداد كفاءة الازالة تتحقق عند اقل تدفق للتتراسايكلين ، اعلى ارتفاع للحشوة، اعلى تركيز للتتراسايكلين واعلى حد لتدفق الهواء. ايضا تم ايجاد علاقة رياضية للحد الادنى من سرعة التميع ووجد انها دالة من سرعة السائل ، حجم حبيبات المادة المازة ، عمق الحشوة وايضا كثافة الجسيمات . ايضا برج الامتزاز المتميع الدوار يحقق اداء افضل بزيادة الوقت اللازم للاشباع بحدود ساعتين مقارنة ببرج التميع التقليدي.

الكلمات الدالة: تيتراسايكلين، سرعة التميع الصغرى، منحنى الاختراق